International Journal of Engineering and Geosciences
https://dergipark.org.tr/en/pub/ijeg
e-ISSN 2548-0960

Reconstruction of Historical Buildings Using Social Media Data: A Case Study from the World Cultural Heritage List

Nursu Tunalioglu [1], Bahattin Erdogan [1], Taylan Ocalan [*1], Duygu Arican [1], Cemali Altuntas [1], Tumay Arda [1], Ali Hasan Dogan [2], Elif Zeynep Arikan [1]

[1] Yildiz Technical University, Department of Geomatic Engineering, Türkiye, ntunali@yildiz.edu.tr, berdogan@yildiz.edu.tr, tocalan@yildiz.edu.tr, duyguaricann@gmail.com, cemali@yildiz.edu.tr, tarda@yildiz.edu.tr, elifzeyneparikan@gmail.com
[2] Tokat Gaziosmanpasa University, Department of Geomatics Engineering, Türkiye, alihasan.dogan@gop.edu.tr

Cite this study: Tunalioglu, N., Erdogan, B., Ocalan, T., Arican D., Altuntas, C., Arda T., Hasan Dogan, A., Zeynep Arikan, Elif.. (2026) Reconstruction of Historical Buildings Using Social Media Data: A Case Study from the World Cultural Heritage List. International Journal of Engineering and Geosciences, 11 (1), 21-39.

https://doi.org/10.26833/ijeg.1635501

Keywords
Crowdsourced Data
Social Media Platforms
Structure-from-Motion (SfM)
3D Modeling
Cultural Heritage

Research Article

Received:07.02.2025
Revised: 24.032025
Accepted:07.04.2025
Online Published:10.08.2025
Published:01.02.2026

Abstract

Cultural and natural heritage assets, as a set of tangible and intangible values that reveal the shared past and historical accumulations of the communities living together, are important not only for the past but also for the transfer to future generations and are the responsibility of all nations of the world. Today's digitalized information age, development, and change in science and technology contribute to producing highly accurate three-dimensional (3D) inventories of these cultural heritages. However, in addition to natural degradation and destruction processes, unexpected events such as war, terrorist attacks, and natural disasters can hinder the formulation of the traditional inventories. At this point, it is important to carry out 3D modeling studies using crowdsourced images and videos from social media, to enhance modeling accuracy and support digital documentation, virtual museum initiatives, and heritage preservation. This study aims to present a strategy following the Structure-from-Motion approach to create 3D models of cultural heritage assets by using shared crowdsourced images and videos collected via social media platforms and applying a normalization procedure for scale standardization to assess model accuracy. Data obtained during nighttime, snowy conditions, or overly filtered captures were excluded, and a segmentation procedure using the Segment Anything model was implemented to remove irrelevant objects. As a result, an approach that can be used in inventory studies has been presented by using images and videos shared by users on social media platforms through an integrated and mutually supportive methodology. Quantitative analysis using the M3C2 method showed that RMSE values ranged from 0.0010 to 0.0036 across the models, with over 93% of the matched points falling within ±1σ. These results confirm the reliability of the proposed approach for large-scale digital heritage documentation.

1. Introduction

While various artifacts and social values that have physically existed from the past to the present contribute to the formation of cultural heritage, transferring these values to future generations is crucial for society to recognize its history, identity, and culture [1]. Today, cultural heritage faces threats from various factors, including natural disasters, civil wars, terrorist attacks, and vandalism. The virtualization of cultural heritage items ensures their digital protection and facilitates their transmission to future generations. As the importance of three-dimensional (3D) modeling applications grows, various methods that utilize different technologies to produce digital models have been documented in the literature [2-4].

The most used methods in the 3D modeling of cultural heritage include laser scanning, photogrammetry, Unmanned Aerial Vehicles (UAVs) and computer vision techniques [5]. Yakar [6] examined the usability of UAVs in documenting cultural heritage. By replacing traditional methods with modern technologies, UAVs

provide an effective and accurate approach to heritage documentation, ensuring the preservation of cultural assets for future generations. With laser scanners, it is possible to generate dense 3D point clouds and high-resolution geometric models of objects, although the desired color quality is not always achievable. In photogrammetry, on the other hand, the 3D geometry of objects is constructed using high-resolution images. Kadobayashi et al. [7] explored the integrated use of laser scanning and photogrammetry methods in their study, achieving results with 1 mm accuracy. The study highlighted the importance of such models for preserving cultural heritage, enabling faithful restorations, and providing interdisciplinary solutions. Şasi & Yakar [8] presented the 3D photogrammetric modeling of Sakahane Masjid, a historical artifact from the Anatolian Seljuk era in Konya. Using a Nikon D90 camera and a DJI Phantom 4 UAV, photographs were captured and processed with Agisoft PhotoScan to create detailed 3D models. Uslu & Uysal [9] focused on the 3D modeling of the Demeter Statue in the Kütahya Archaeology Museum using terrestrial photogrammetry. Control points on the statue were measured with a reflectorless total station, and photographs were captured using a Nikon Coolpix P510 camera. The findings demonstrated the advantages of photogrammetry in archaeological documentation, providing accuracy, speed, cost efficiency, and versatility for preserving cultural heritage. Ulvi et al. [10] focused on the photogrammetric survey of Kızıl Kilise, located in the Sivrihisar village of Güzelyurt district in Aksaray. By employing digital photogrammetry techniques, scaled drawings, 3D models, and point clouds of the church's exterior were produced. The research highlights how advancing photogrammetry technologies provide time- and cost-effective solutions for documenting and preserving cultural heritage. However, these methods require high costs, labor, expertise, and technological resources, which may hinder their continuous use. Varol [11] emphasized the importance of UAV photogrammetry in creating detailed and accurate cultural heritage inventories. The study demonstrated that high-resolution 3D models and orthophotos generated using UAVs can significantly enhance the documentation and classification of heritage sites. Moreover, Yakar et al. [12] emphasized the importance of 3D documentation in the inventory and preservation of cultural heritage, demonstrating the effectiveness of terrestrial laser scanning for accurate data acquisition.

Technological developments in the field of photogrammetry and computer vision techniques have provided a new set of tools that allow 3D modeling of cultural heritage items [13]. In addition to traditional photogrammetric methods, recent Artificial Intelligence (AI)-driven approaches such as Neural Radiance Fields (NeRF) and deep learning-based super-resolution techniques have introduced new possibilities in 3D reconstruction. NeRF has been effective in synthesizing photorealistic 3D representations, yet it is computationally demanding and typically requires high-quality input images with consistent viewpoints [14]. Similarly, deep learning-based super-resolution techniques enhance image details but do not inherently reconstruct 3D structures [15]. While these methods provide advantages in specific scenarios, their applicability to large-scale and unstructured image datasets, such as those obtained from social media, remains limited. The Structure-from-Motion (SfM)-based approach is more suitable for handling crowd-sourced, variable-quality images without requiring large-scale training datasets [16, 17]. SfM algorithm allows the production of high-quality 3D models of objects using two-dimensional (2D) images. Herman et al. [18] have created a 3D model of Romanian wooden churches using images obtained by photogrammetry methods. The conclusion of the study has shown that photogrammetry, which offers the advantage of lower resource usage in 3D model production compared to laser scanning methods, may be used in future research. Deliry & Avdan [19] emphasized the effectiveness of Unmanned Aerial Systems (UAS) combined with SfM for rapid and accurate topographic surveying. By analyzing flight height, Ground Control Points (GCPs), and software, the research demonstrated that optimized UAS-SfM workflows can produce high-accuracy 3D models and digital surface models, offering a cost-effective alternative to traditional methods. Bakirman & Gumusay [20] explored the integration of body motion with a custom Street View service created for Yildiz Technical University Davutpasa Campus using Microsoft Kinect and Flexible Action and Articulated Skeleton Toolkit. By leveraging Google Maps Application Programming Interface and panoramic images, the research demonstrated a low-cost approach to virtual reality, offering applications for virtual museums, heritage sites, and planetariums.

Cultural heritage items have suffered irreversible damage due to wars, terrorist attacks, and deliberate destruction. In war zones, security threats and limited access have made fieldwork impossible. This has led researchers to explore new data sources for digital reconstruction of structures. Documenting cultural heritage using internet archives has become a popular research topic. Grün et al. [21] investigated the utility of archived images in the physical reconstruction of a structure in Afghanistan that no longer exists due to the deliberate destruction of 1700-year-old Buddha statues by Taliban forces in 2001. Grussenmeyer & Al Khalil [22], succeeded in creating 3D geometric solutions by creating a photogrammetric archive of a 900-year-old mosque that was severely damaged in the clashes during the Syrian war. In 2015, the Mosul project (namely Rekrei) was launched for the digital restoration of damaged artifacts after videos of ISIS destroying the Mosul Museum in Iraq, which contains many artifacts dating back to 2500 years ago, were shared on the Internet.

Research has shown that the use of crowdsourced data has yielded successful results in the 3D reconstruction of structures that no longer exist in physical form today [23-25]. The Plate Stone Bridge Project [26] is an example of this. After the collapse of the largest stone bridge in the Balkans due to heavy rains in 2015, volunteer groups created by the National Technical University of Athens used crowdsourced data to model the bridge's original shape and size before its collapse. The use of crowdsourced data reduces the resource

requirements in projects by a significant amount, but the data obtained is not always sufficient to create a 3D model, so it is recommended to integrate as much data as possible.

Crowdsourced data can be provided by volunteer groups or data captured by tourists and shared on social media platforms. Today, there are numerous projects based on the use of crowdsourced data with the cooperation of different institutions and non-governmental organizations. For instance, the Heritage Together project [27] aims to document cultural heritage in partnership with local communities, while the Zamani Project collaborates with international heritage organizations to create a digital heritage collection, intending to promote the recognition and preservation of heritage items by the public. Image-based 3D model production with the use of crowdsourced social media data provides advantages in terms of low cost and manpower requirements and minimizing fieldwork. In addition, domestic studies have also shown that crowdsourced data can effectively document cultural heritage. Uslu & Uysal [28] used Flickr images for 3D documentation of the Afrodisias Tetrapylon, and Uslu & Uysal [29] reconstructed the Trojan Horse using UAV data with SfM.

To understand and validate models generated from different data sources, it is essential to register them within a common reference system [24]. While this process is straightforward for existing structures, it becomes significantly more challenging for artifacts that no longer exist due to the absence of direct reference points. This paper presents an approach to create digital models of structures and to evaluate the accuracy of models generated using crowdsourced data from social media. Generally, 3D models are compared to a reference model, which is assumed to be more accurate than the others. However, due to the use of diverse data sources and the absence of GCPs, this study introduces a normalization method to ensure comparability across models. Specifically, all models were normalized along three axes to achieve a uniform scale. This method addresses a challenge in multi-source 3D modeling and offers a more flexible, scalable approach for validating models derived from crowdsourced data. In this context, 3D models were created for prominent historical landmarks, including the Holy Trinity Column in the Czech Republic, Roskilde Cathedral in Denmark, the rock-cut tombs of El Hazne in Petra, Jordan, and the Bode Museum located on Berlin's Museum Island, which are listed on the UNESCO World Heritage List. As data sources, publicly available images and videos from popular platforms like Instagram, Twitter, Facebook, and YouTube were collected.

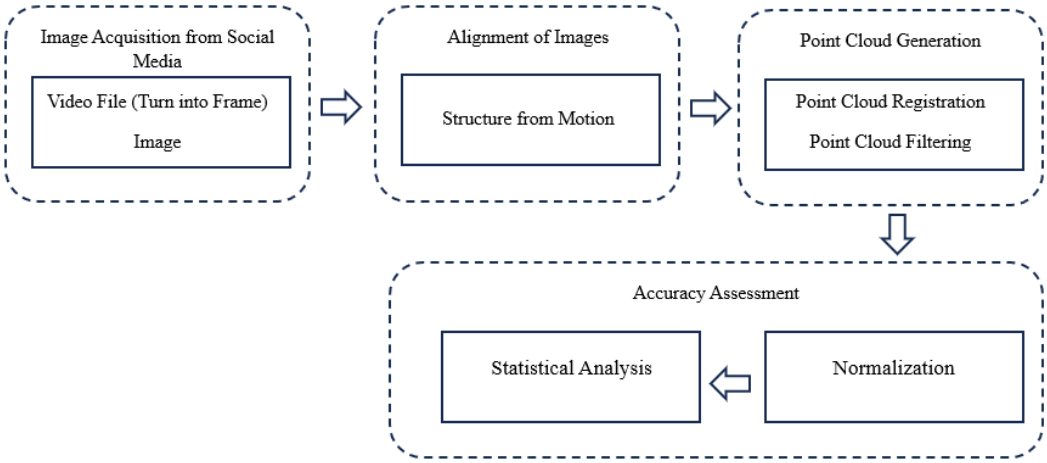

Figure 1. Study workflow

2. Methodology and Case Study

This section focuses on the techniques and methods employed in the study, followed by a description of the data and study area. Finally, the analysis is presented.

2.1. Methods

This study aims to create 3D models of cultural heritage structures using crowdsourced aerial and terrestrial videos and images from social media, incorporating location and time tags. Therefore, the study areas were chosen from cultural and natural assets on the UNESCO World Heritage List. The integration of data from different social media platforms is a critical component of the study. This involves the incorporation of data from various acquisition principles and resolutions. In general terms, the study includes the acquisition of data, quality control, classification, generation of the integrated model, and assessment of the results. Using the datasets produced within the scope of the study, 3D point cloud models were produced by photogrammetric evaluation based on SfM. Figure 1 summarizes the steps followed in the workflow diagram. Detailed information regarding methods applied is given in the following subsections.

2.1.1. Segment Anything Model (SAM)

In this study, the Segment Anything Model (SAM) was used to remove the background from the images. SAM is an advanced image segmentation model based on state-of-the-art techniques. The model was trained on a

dataset consisting of millions of images and billions of masks. The Segment Anything 1 Billion Mask (SA-1B) dataset, the largest labeled segmentation dataset to date, was explicitly designed for the development and evaluation of advanced segmentation models. SAM can segment objects based on the input provided. SAM consists of three main components: an image encoder, a prompt encoder, and a lightweight mask decoder (Figure 2). In Figure 2, the segmentation prompt (top-left) is passed to the Prompt Encoder, while the image itself (top-right) is processed by the Image Encoder. The Lightweight Mask Decoder then merges these encoded features to generate the final segmentation mask (bottom image), effectively isolating the target object, in this example, the Holy Trinity Column, from the background. This workflow demonstrates how SAM can semi-automatically identify and extract specific elements of interest from a complex scene, thereby simplifying subsequent processing steps in 3D modeling workflows.

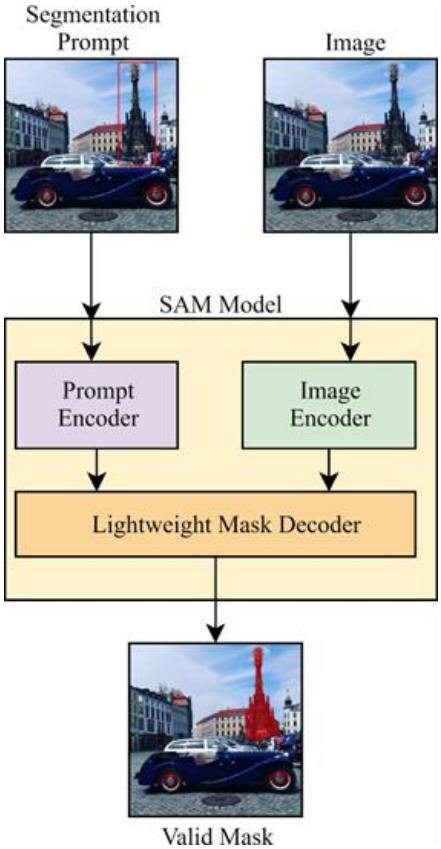

Figure 2. SAM Model (adapted from [30])

The image encoder generates vector profiles of the input images. The prompt encoder processes input data such as points, regions, and text and passes this information to the mask decoder. The mask decoder uses data from the prompt and image encoders to generate three different masks. Here, SAM has been applied to segment the object from the background using region sampling. This approach allows for semi-automatic identification of the object and separation from the background.

2.1.2. Structure from Motion (SfM)

Advanced computer vision techniques such as SfM and Multi-View Stereo (MVS) are being used to predict the position and structure of an object in 3D space using images. SfM algorithms are based on the reconstruction of the scene geometry and the estimation of the camera parameters. The basic principle of the SfM is based on binary vision and estimation of the observed point by a method that uses changing vision from a moving point. Contrary to traditional photogrammetry, the technique does not require GCPs and camera calibration since camera position and orientation are solved together within the model geometry [31, 32]. For this purpose, relative and absolute positions of scene images must be analyzed to determine the relationships between different images [33]. SfM uses distinctive key points of structures to identify and optimize the positions of these points in terms of camera position, orientation, and intrinsic parameters. In this way, it reconstructs the 3D geometry of the scene by defining key features of structures [34, 35].

Compared to traditional photogrammetric approaches and laser scanning, SfM provides a cost-effective and accessible solution, particularly for historical and inaccessible sites where extensive fieldwork may not be feasible. The ability to reconstruct 3D geometry from crowdsourced and publicly available images makes it especially useful for cultural heritage documentation [32, 36]. The method also allows for automated feature extraction and scene reconstruction, making it a flexible alternative to conventional surveying techniques.

The MVS technique, on the other hand, establishes the relationship of measurements made from several images simultaneously. In other words, the SfM algorithm predicts camera movements and object positions using images of objects taken from different angles, whereas the MVS algorithm detects common features between images.

The SfM workflow follows several key steps to achieve an accurate 3D reconstruction [31]:

1. Feature detection and matching – Identifying keypoints in multiple overlapping images using algorithms such as SIFT (Scale-Invariant Feature Transform).
2. Camera pose estimation and bundle adjustment (BA)– Optimizing the relative positions and orientations of images to ensure geometric consistency.
3. Sparse point cloud generation – Establishing a preliminary 3D structure based on feature correspondences.
4. MVS densification – Enhancing the sparse model by generating a dense point cloud representation.
5. Mesh reconstruction and texturing – Converting the dense point cloud into a surface model with detailed textures.

This structured workflow enables automated and scalable 3D model generation, making SfM a robust method for reconstructing historical structures using publicly available imagery. Following these steps, the final 3D model is generated and evaluated using accuracy assessment techniques such as Multiscale Model to

Model Cloud Comparison (M3C2) to ensure reliability before documentation and analysis.

2.1.3. Multiscale Model-to-Model Cloud Comparison (M3C2)

For the accuracy analysis of the created models, the M3C2 method developed by [37] was used, which measures the distance between two points, estimates confidence intervals and compares calculations using synthetic point clouds with existing techniques. When comparing different model results, this method employs scaling and statistical analysis to evaluate the quality and reliability of the generated models. The fundamental principle is the creation of a calculation set called core points, and the use of this set to calculate the M3C2 distance and confidence interval [37]. Unlike other commonly used methods for measuring the distance between two-point clouds in the literature, the M3C2 method directly operates on the point cloud itself, eliminating the need for meshing or gridding [38]. Additionally, it is robust against missing data between scans and variations in point cloud density.

According to the working principle of the algorithm, reference point clouds should be determined first, and then a two-step path is followed, consisting of determining the surface normal on these reference clouds and measuring the distance between two-point clouds along the determined surface normal.

2.1.4. Determination of the Surface Normal

A local model with a radius $D/2$ of the D normal scale is created around the core point i, and the surface normal vector is defined in this local model plane. Although the $D/2$ radius value may be a variable value depending on the user experience, it can be calculated by taking 20-25 times the estimated roughness values from the point cloud. More detailed information can be found in [37].

2.1.5. Determination of the Distance Between Two Point Clouds

A new plane with a radius of $d/2$ is drawn on the projection scale d within the area with the defined normal scale D. $d/2$ has a relatively smaller value compared to the $D/2$ scalar value and can be explained as the reason why the method is called multiscale [39]. The new plane created should be expanded in the direction of the surface normal to form a cylinder. This cylinder encloses both the reference point cloud and the cloud to be compared, so that two subsets of points, n_1 and n_2, are obtained in the area remaining in the cylinder. To calculate the distance between two-point clouds, called the M3C2 distance, the average positions of the n_1 and n_2 subpoint clusters must be calculated. The M3C2 distance is equal to the distance between the average positions. The smoothness of the point cloud around the core point is calculated as the standard deviation of the distances between points on the D normal scale. For each distance measurement, a confidence interval is defined based on the smoothness of the point cloud and registration errors. As a result, the measurement of two-point clouds in the M3C2 algorithm requires the following parameters [40].

- Determination of the point cloud to be compared with the reference point cloud
- Definition of the core point
- Definition of Normal Scale (D), projection scale (d) and cylinder depth
- Identification of the registration error

2.2. Study Areas and Data Collection

Cultural heritages are selected based on their architectural differences, structural features, number of visitors, and the amount of data that can be obtained through social media platforms. The selected study areas are the Holy Trinity Monument in the Czech Republic, Roskilde Cathedral in Denmark, Bode Museum in Germany, and the ancient city of Petra in Jordan. The Holy Trinity Monument in Olomouc, Czech Republic, reflects the rich detailed baroque architecture. At the same time, Roskilde Cathedral on Zealand Island, Denmark, is characterized by the smooth geometric outlines and monochromatic façade design of Gothic architecture. The Bode Museum in Berlin is surrounded by water, allowing for photography from different perspectives. The rock-cut tomb in Petra, Jordan, called “El-Khazneh” or “The Treasure”, is multicolored and dynamic because it is carved out of sandstone rock with various shades of pink, red, yellow, orange, and other colors depending on the angle at which the sunlight falls on it, and the inability to capture 360-degree views of its surroundings makes it necessary to investigate whether modeling can be accomplished.

The data on the cultural heritage addressed in the study were obtained from social media platforms such as Facebook, Twitter, Instagram, YouTube, Flickr, and TripAdvisor. Images and videos shared on these platforms publicly available by users were classified separately for each cultural heritage and four inventories were created. The temporal resolution determined for these four inventories is planned to cover one year between 01.01.2022 and 01.01.2023. The main reason for choosing a temporal resolution of one year is the definition of [41], which includes “... the threat of extinction due to natural degradation, major changes due to unknown causes, abandonment of an asset for any reason; the outbreak of an armed conflict or the threat of conflict; disasters and catastrophes; the threat of serious and significant hazards such as serious fires, earthquakes, landslides, volcanic eruptions; changes in water level, floods and tidal waves...” elements may cause structural changes and consistency in the data obtained was ensured. However, a sufficient number of images and videos could not be obtained during the data collection process in the specified one-year period. Therefore, the data duration was extended. Although it was desired to extend the duration while maintaining the up-to-date data, the travel restrictions imposed by the Covid-19 outbreak, which was declared a pandemic by the World Health Organization on March 11, 2020, negatively affected tourism and therefore cultural heritage visits, which led to a decrease in social media posts.

Considering this situation, data was collected by extending the period until April 2024.

2.3. Analysis

The initial search analysis was a crucial step in our process, as it provided valuable insights into the type and quantity of data available. We found that queries related to location and structural attributes generated a significant number of results. The assessment of these search results highlighted several factors that influenced the quantity and quality of the usable data. The quality of the data was often compromised by posts with inaccurate or inconsistent tagging, nighttime photos with dark areas, and excessive use of filters on images. In the analysis section and later in the study, datasets will be abbreviated and referred to as "DS" to improve readability and indicate the datasets used in the study. Taking these factors into consideration, we constructed the DSs, which are presented in Table 1. By incorporating publicly available images and videos from all social media platforms, along with posts from private accounts, we were able to significantly increase the number of search results.

In the obtained images and videos, both temporal consistency and alignment with the relevant inventory were considered. Upon examining these conditions, it was observed that the relevant inventory is inconsistent in the images and videos shared on social media due to the factors listed above. To ensure the highest data quality, a rigorous manual quality check was performed during the initial screening stage, leading to the exclusion of inconsistent data. For temporal consistency, the date of sharing on social media platforms was taken into account for the images and videos. This consideration includes situations where older images or videos are shared as current within the defined range. Additionally, images and videos are shared using hashtags like #tbt or #ThrowbackThursday, which is part of the Throwback Thursday trend on social media.

Image backgrounds were segmented and masked using the SAM model to minimize any potential impact on point cloud generation and enhance the accuracy of the resulting 3D model. Images and data accessible through social media platforms were downloaded using the time range and tags specified in Table 1.

For data integration, the DSs have been designated as A for image-based data, B for images generated from videos, and C for cases where both A and B DSs are considered together. In this context, DS-A and DS-C were considered when generating point clouds.

A three-stage approach was followed in the creation of the 3D model. Accordingly, the models created using raw, unprocessed images and videos are designated as Model 1 (M-1). Models obtained by eliminating the effects that could compromise the integrity of the subject in the raw DSs (such as nighttime, snowy, and filtered images) are designated as Model 2 (M-2). Models derived from applying the SAM to the images in Model 2 are designated as Model 3 (M-3). All DSs classified were processed using the SfM method with the open-source software VisualSFM to obtain point clouds. To ensure optimal keypoint detection and matching, the SIFT algorithm was utilized, allowing for robust feature extraction across varying lighting conditions. The camera calibration parameters, including focal length and lens distortion, were estimated automatically within the VisualSfM workflow. Additionally, BA optimization process was performed to refine camera positions and improve overall accuracy.

The resulting sparse point cloud was then processed through MVS to generate a dense point cloud. The Patch-based Multi-View Stereo (PMVS) algorithm was used for this process.

Accordingly, point cloud models obtained using the raw data designated as DS-1A and DS-1C (M-1, A-C; M-2, A-C; M-3, A-C) are presented in Figures 3-6 for the Holy Trinity Column, Roskilde Cathedral, Bode Museum, and Petra, respectively. In Figures 3-6, subfigures (a) through (f) illustrate how incremental filtering and SAM-based segmentation progressively enhance point cloud quality.

The obtained raw point cloud models were subjected to the filtering process using the open-source software CloudCompare. A three-stage filtering approach was followed consecutively. Accordingly, (1) noise selection and filtering through segmentation based on RGB color codes (Colorimetric Segmenter), (2) noise filtering (Noise Filter), and (3) manual filtering were applied. The model representations obtained as a result of the filtering processes were presented using Model-1C for each structure to avoid redundancy. The point clouds obtained at each filtering step and the results are shown in Figures 7-10 for the Holy Trinity Column, Roskilde Cathedral, Bode Museum, and Petra, respectively. As illustrated in figures, each subfigure shows the incremental removal of unwanted points at each filtering stage, ultimately providing a refined point cloud. The color-coded areas highlight which points were removed or retained to provide a clear visualization of the progressive cleaning process for each structure.

Table 1. Data and attributes obtained from social media platforms

Structure	Social Media Platform	Location Tag	Attribute Tag	# Videos	# Images	Resolution Range (Pixel)/ Video FPS Range
Holy Trinity Column (Czechia)	Facebook	Olomouc	Holy Trinity; Holy Trinity Column; Holy Trinity Column Olomouc	3	41	720-1080/ 25-30
	Instagram	-	Sloupnejsvetejsitrojice; holytrinitycolumn	5	428	
	Twitter	Olomouc, Chechzia	Holytrinity; holytrinitycolumn	-	45	
	Youtube	-	Holy Trinity Column; Holy Trinity Column in Olomouc; Olomouc; Holy Trinity Column in Czech Republic	32	-	
	TripAdvisor	Olomouc, Chechzia	Holy Trinity Column	-	33	
Roskilde Cathedral (Denmark)	Facebook	Roskilde Cathedral Roskilde Domkirke Roskilde Katedrali	Roskildedomkirke; roskildecathedral	5	96	720-1080/ 25-30
	Instagram			19	715	
	Twitter			3	39	
	Youtube			24	-	
	Flickr			-	28	
	TripAdvisor			-	45	
Bode Museum (Germany)	Facebook	Bode Museum Berlin Museum Island Müzeler Adası	Bodemuseum; museumisland	-	30	720-1080/ 25-30
	Instagram			15	450	
	Twitter			-	38	
	Youtube			33	-	
	Flickr			-	84	
	TripAdvisor			-	50	
Petra (Jordan)	Facebook	Petra; Ürdün	Petra; Petra Jordan	5	159	720-1080/ 25-30
	Instagram	-	petrajordania	20	1201	
	Twitter	Jordan	Petra; petrajordan	6	54	
	Youtube	-	Petra; Petra Ürdün; Petra Jordan; El-Hazne; El-Hazne Petra; Al-Khazneh; Al-Khazneh Petra; Petra Hazine Binası	35	-	480-1080/ 25-30

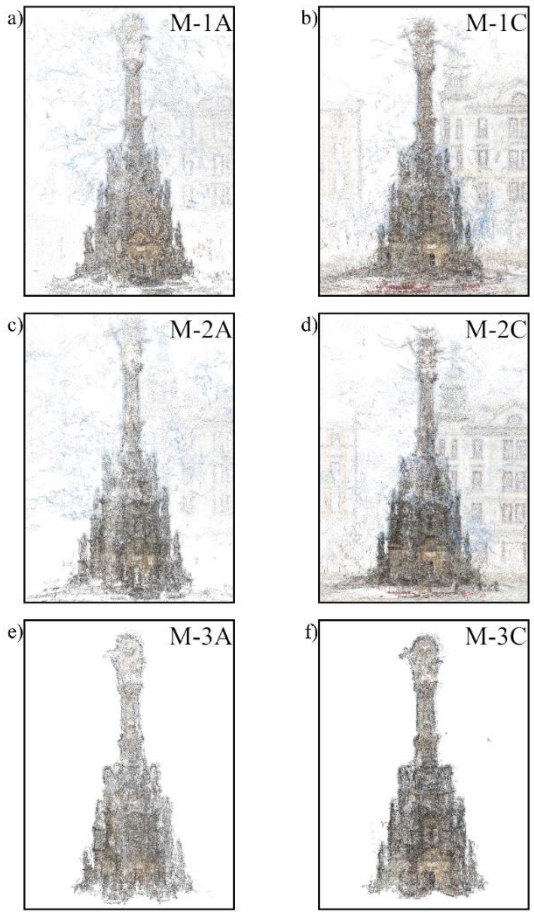

Figure 3. Holy Trinity Column - raw point clouds generated for M-1, M-2, and M-3 using images (A) and images+videos (C)

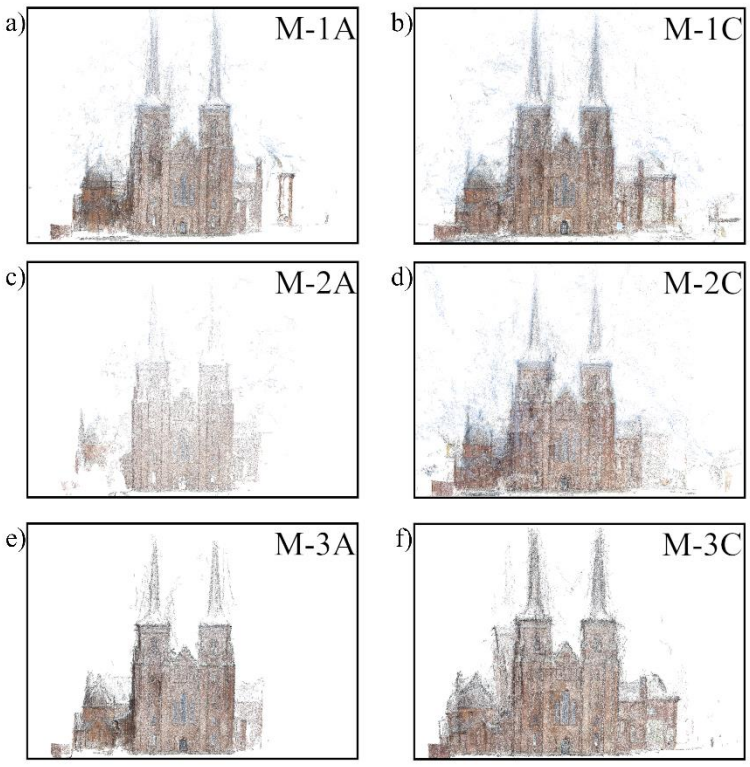

Figure 4. Roskilde Cathedral - raw point clouds generated for M-1, M-2, and M-3 using images (A) and images+videos (C)

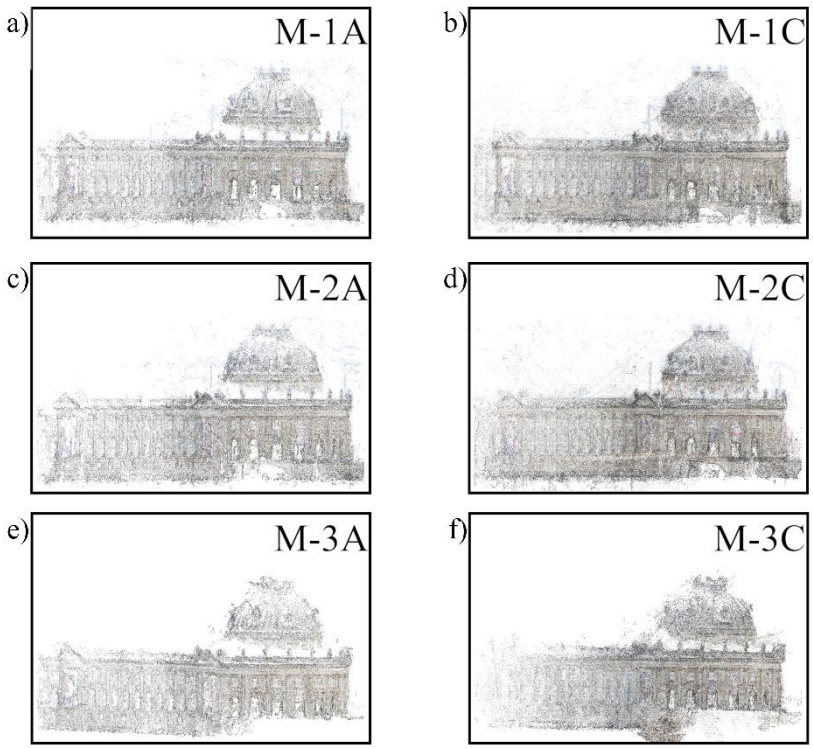

Figure 5. Bode Museum - raw point clouds generated for M-1, M-2, and M-3 using images (A) and images+videos (C)

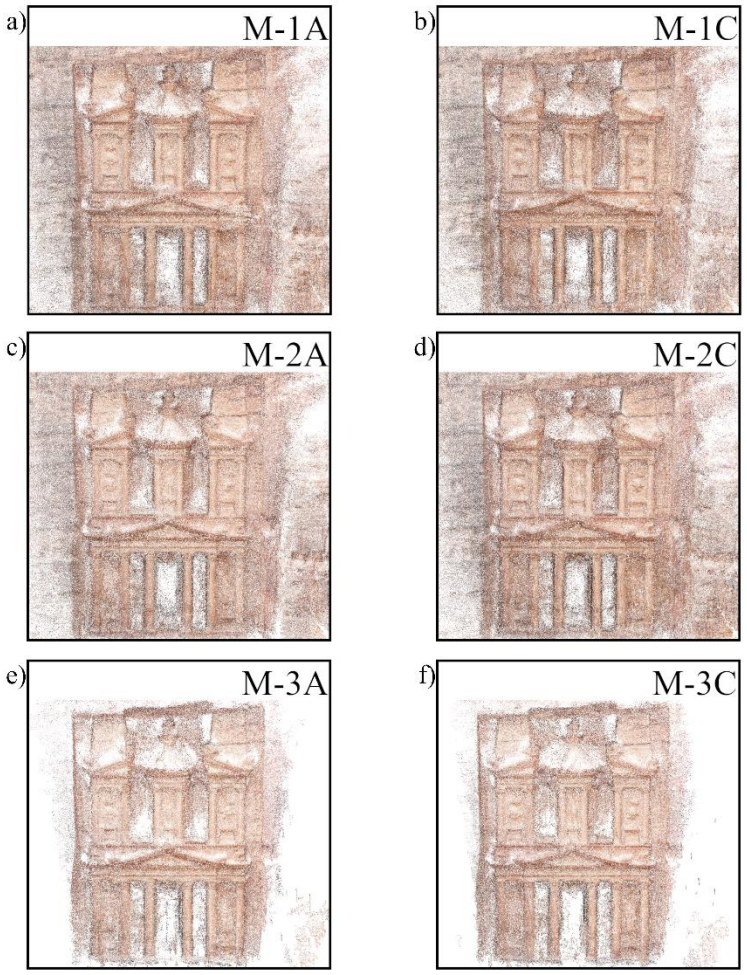

Figure 6. Petra - raw point clouds generated for M-1, M-2, and M-3 using images (A) and images+videos (C)

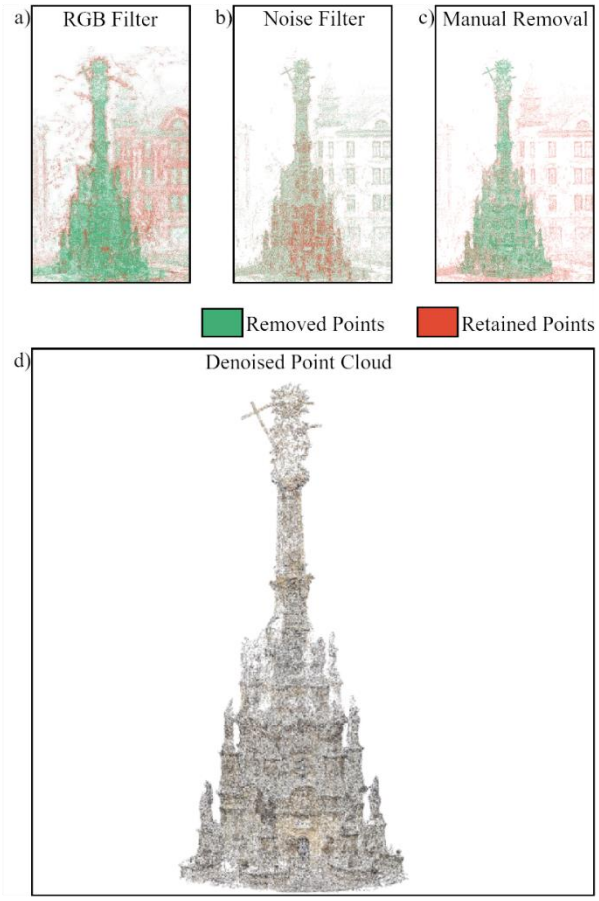

Figure 7. Filtering process and result for Holy Trinity

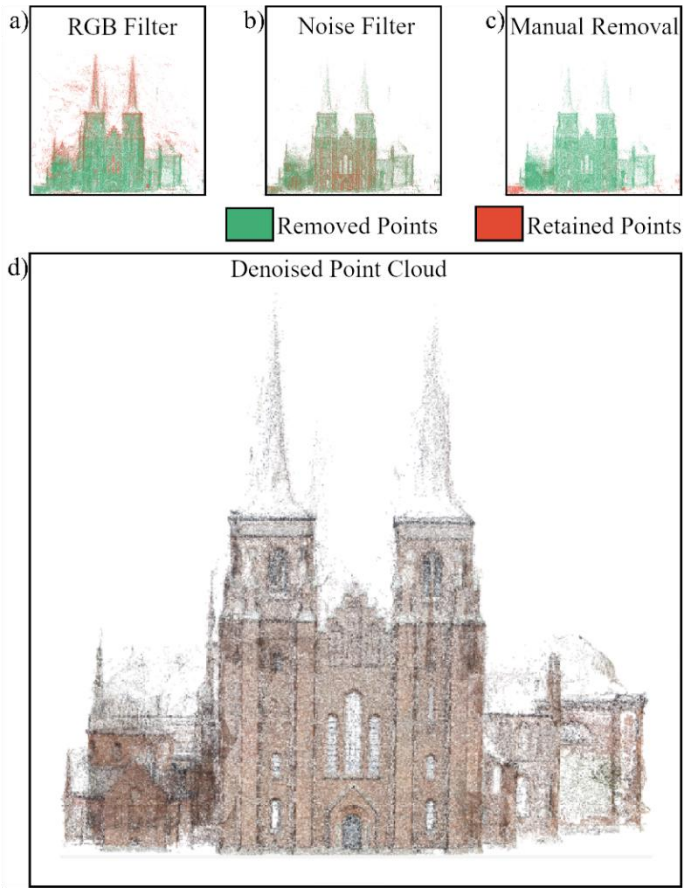

Figure 8. Filtering process and result for Roskilde Cathedral

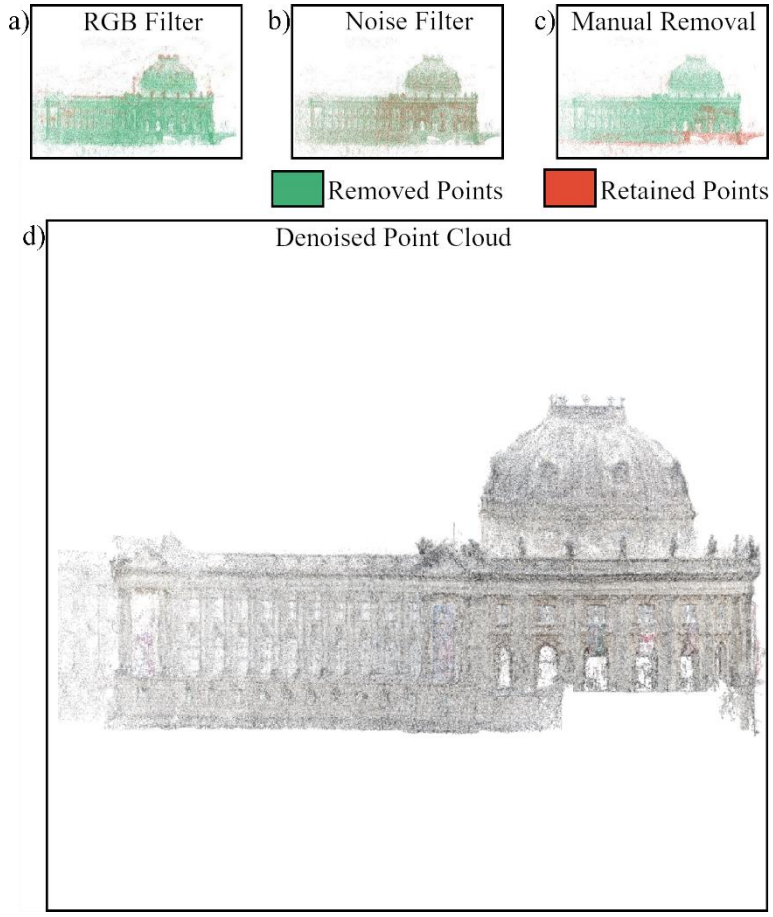

Figure 9. Filtering process and result for Bode Museum

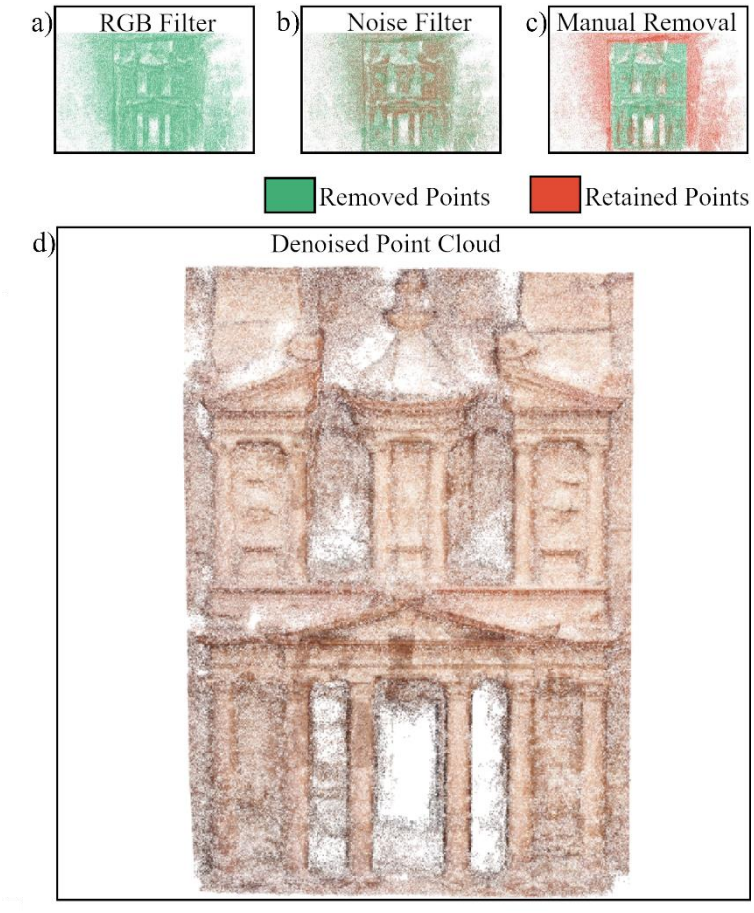

Figure 10. Filtering process and result for Petra

The models represented in Figures 7-10 are also used as reference to compare with the other models for statically assessing the performance of the crowdsourced data supported via social media. Figures 11-14 show the M3C2 comparisons and difference intervals for the Holy Trinity Column, Roskilde Cathedral, Bode Museum, and Petra, respectively. For each structure, equal intervals are provided along the negative-to-positive range: -1.0, -0.5, 0.0, 0.5, 1.0 for the Holy Trinity Column, -6.0, -3.0, 0.0, 3.0, 6.0 for Roskilde Cathedral, -1.5, -0.75, 0.0, 0.75, 1.5 for the Bode Museum, and -0.7, -0.35, 0.0, 0.35, 0.7 for Petra. These intervals illustrate the extent of deviations between point clouds in a uniform manner. Hereinafter, noise-filtered point clouds have been presented and designated as MP.

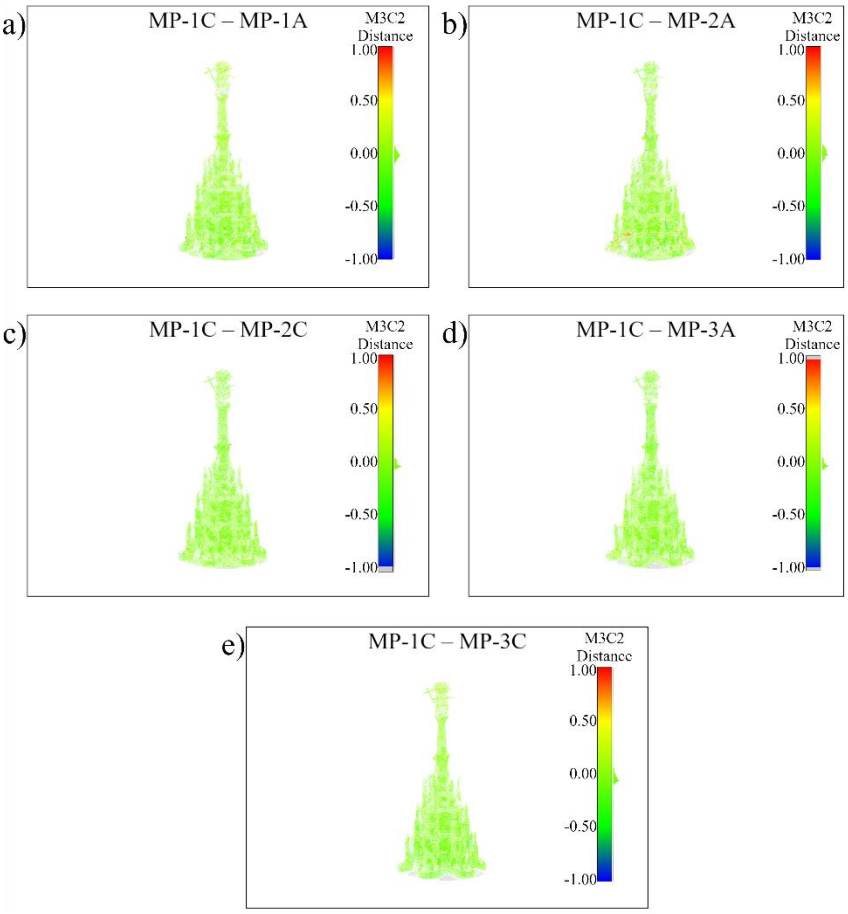

Figure 11. The M3C2 difference for Holy Trinity Column

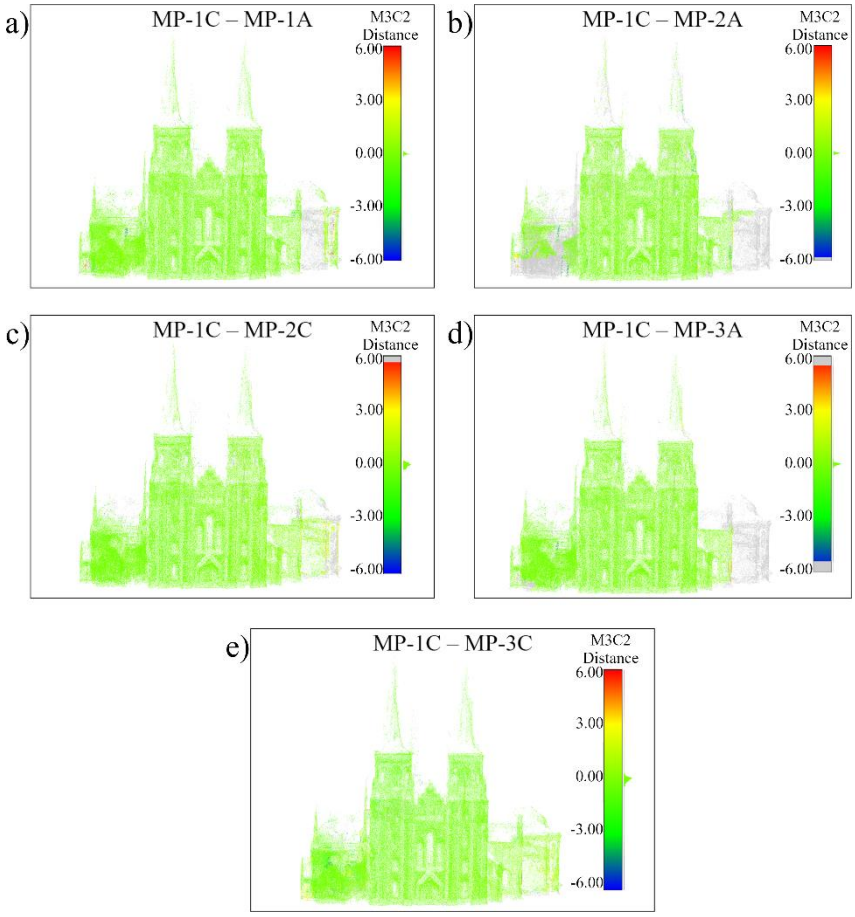

Figure 12. The M3C2 difference for Roskilde Cathedral

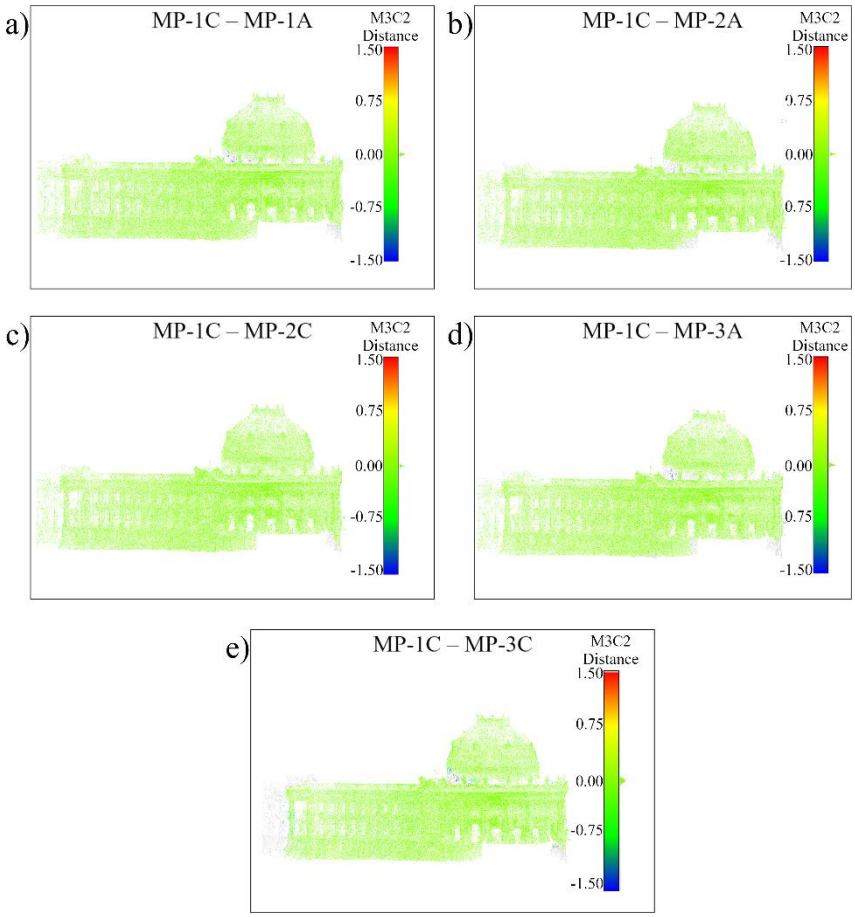

Figure 13. The M3C2 difference for Bode Museum

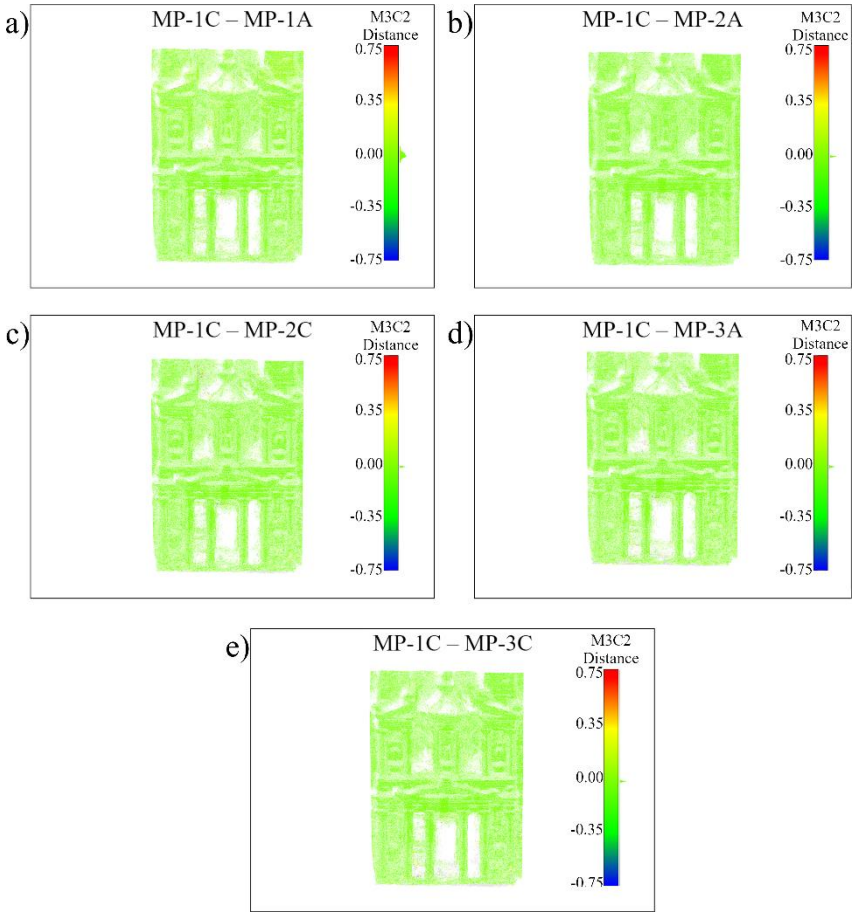

Figure 14. The M3C2 difference for Petra

3. Results and Discussion

The statistical results obtained for four structures with distinct architectural features are presented in Table 2. The study aims to create inventories of cultural heritage through the evaluation of data sourced from different social media platforms on a crowdsourcing basis. Therefore, ensuring structural integrity without GCPs and irrespective of metric size measurements is conducted. This allows for the comparison of models obtained under different scenarios, but it does not allow the evaluation of comparative difference values between the structures. In other words, the variations among the models depend not on the metric properties of the structures but on the size of the structure itself. To overcome this issue and perform this evaluation within the scope of the study, a scaling factor based on the dimensional size of each structure obtained through SfM along three axes has been calculated. The scaling factors are as follows: 1/14.94 for the Holy Trinity Column; 1/78.36 for Roskilde Cathedral; 1/26.63 for the Bode Museum; and 1/9.62 for Petra. The statistical results presented in Table 2 are scaled values and are given in unitless terms. Table 2 includes the RMSE values and standard deviations. RMSE values were calculated based on the differences. However, standard deviations were obtained around the means of the differences. The lowest RMSE and standard deviation values for the Holy Trinity Column were obtained as 0.0036 between the reference model and the MP-2C model. Here, the MP-2C point cloud model was obtained using source data generated from filtered images and videos. In the comparison, the minimum difference was calculated as -0.0637, the maximum difference as 0.0677, and the range as 0.1314. The next lowest RMSE and standard deviation values were obtained from the comparison with the MP-3A model, which used only image data and underwent a filtering procedure followed by the application of SAM. The effect of SAM in modeling appears to be relatively lower model deviations (minimum difference -0.0652, maximum difference 0.0649, range value 0.1301). For Roskilde Cathedral, the lowest RMSE values of 0.0038 were obtained from the comparison of the reference model with the MP-3A model and the MP-1A model (0.0035), which both used only image data post-filtering procedure. Here, in the MP-3A comparison, the minimum difference was -0.0692, the maximum difference 0.0704, and the range value 0.1395. The Bode Museum has a data set with a high density of data sourced from social media platforms, which has been effective in model comparison accuracy. In the M3C2 comparison conducted, the lowest RMSE and standard deviation values were 0.0010, with a minimum difference of -0.0569, a maximum difference of 0.0617, and a range of differences of 0.1186 achieved with the MP-2C point cloud. The source data used for creating MP-2C involved images and videos combined and subjected to a noise filtering procedure. The application of the SAM algorithm here resulted in a relatively smaller range of differences. Finally, in the modeling study conducted in the Petra site, the model created using source data obtained from images with a noise filtering procedure exhibited the lowest model deviation values. Here, the RMSE and standard deviation

values were 0.0016, with a minimum difference of -0.0752, maximum value 0.0949, and the range of differences 0.1701.

Overall, the comparative analysis of the models demonstrated that accuracy varied based on data density and quality. Among all models, the lowest RMSE was observed for the Bode Museum (0.0010), indicating the highest geometric precision. However, the Petra model exhibited the highest percentage of matched points within ±1σ (96.30%), suggesting superior consistency in structural accuracy. These findings highlight that while RMSE is a crucial metric for assessing geometric precision, the distribution of matched points also plays a significant role in evaluating overall model reliability. Therefore, depending on the evaluation criteria, both the Bode Museum and Petra models can be considered the most accurate representations within this study.

Table 2. Statistical results of M3C2 differences of the structures

Cultural Heritage	Reference Model	Compared Model	Statistics					
			Mean	Std.	RMSE	Min.	Max.	Range
Holy Trinity Column	MP-1C	MP-1A	-0.0010	0.0059	0.0060	-0.0790	0.0731	0.1520
		MP-2A	0.0004	0.0068	0.0068	-0.0721	0.0880	0.1601
		MP-2C	-0.0006	0.0036	0.0036	-0.0637	0.0677	0.1314
		MP-3A	-0.0007	0.0049	0.0049	-0.0652	0.0649	0.1301
		MP-3C	-0.0018	0.0051	0.0054	-0.0737	0.0747	0.1484
Roskilde Cathedral	MP-1C	MP-1A	-0.0002	0.0035	0.0035	-0.0779	0.0832	0.1611
		MP-2A	0.0002	0.0064	0.0064	-0.0746	0.0830	0.1576
		MP-2C	0.0006	0.0049	0.0049	-0.0764	0.0725	0.1489
		MP-3A	0.0003	0.0038	0.0038	-0.0692	0.0704	0.1395
		MP-3C	0.0000	0.0096	0.0096	-0.0869	0.0893	0.1762
Bode Museum	MP-1C	MP-1A	-0.0001	0.0019	0.0019	-0.0677	0.0907	0.1584
		MP-2A	0.0000	0.0016	0.0016	-0.0676	0.0593	0.1269
		MP-2C	0.0000	0.0010	0.0010	-0.0569	0.0617	0.1186
		MP-3A	0.0000	0.0015	0.0015	-0.0758	0.0583	0.1341
		MP-3C	0.0000	0.0027	0.0027	-0.0621	0.0556	0.1177
Petra	MP-1C	MP-1A	0.0012	0.0037	0.0039	-0.1010	0.1000	0.2010
		MP-2A	0.0000	0.0016	0.0016	-0.0752	0.0949	0.1701
		MP-2C	0.0001	0.0025	0.0025	-0.0933	0.0893	0.1826
		MP-3A	0.0001	0.0030	0.0030	-0.1018	0.1007	0.2025
		MP-3C	0.0002	0.0027	0.0027	-0.1029	0.0948	0.1977

In Table 3, statistical analysis regarding the distribution of the M3C2 differences for each structure are presented. With 1,083,656 matched points, MP-2C is the model, which has been compared by the highest number of matched points for the Holy Trinity Column. According to the percentages of the matched points in the comparison and the standard deviations of the differences, the distribution of the point numbers was found as 93.26% between ±1σ, 98.40% between ±2σ, 98.80% between ±3σ and 1.20% equal or greater than ±3σ. For the case of Roskilde Cathedral, although the MP-1A model has the highest number of matched points, the best results were obtained by the MP-3A model. The distribution of the point numbers of the MP-3A model was found to be 95.79% between ±1σ, 98.80% between ±2σ, 99.08% between ±3σ and 0.92% equal or greater than ±3σ. In the case of the Bode Museum, the best results were yielded by the MP-1A model, and the distribution of the point numbers was found as 96.16% between ±1σ, 98.60% between ±2σ, 99.14% between ±3σ and 0.86% equal or greater than ±3σ. Considering the other structures, the lowest standard deviations of the averages of the model differences were obtained for the case of Bode Museum in all model comparisons. For Petra, the best results were obtained by the MP-2A model, and the distribution of the point numbers was found as 96.30% between ±1σ, 98.94% between ±2σ, 99.45% between ±3σ and 0.55% equal or greater than ±3σ.

Selecting an appropriate 3D reconstruction method for cultural heritage documentation requires a careful evaluation of cost, accuracy, and scalability. A comparison between crowd-sourced 3D reconstruction, laser scanning, and UAV photogrammetry highlights notable distinctions. Laser scanning delivers sub-millimeter accuracy but requires expensive equipment and direct access to heritage sites, making it less feasible for inaccessible locations [23]. UAV photogrammetry balances cost and precision; however, it still depends on structured data collection and controlled flight paths [42]. In contrast, the crowdsourced approach provides a cost-effective and scalable alternative, particularly valuable for documenting inaccessible, endangered, or lost heritage sites. Despite challenges related to image quality and viewpoint inconsistencies, its ability to leverage widely available social media data offers a unique advantage in large-scale heritage documentation.

While this study does not incorporate real-time data integration, future research could explore its potential benefits for cultural heritage documentation. Continuously updating 3D models with newly available social media images and videos could enhance reconstruction accuracy while enabling the monitoring of structural changes over time [43]. This approach has

been demonstrated in studies utilizing historical image archives and crowdsourced UAV imagery to reconstruct lost heritage sites digitally and monitor structural changes through sequential updates. Such an approach would be particularly useful for assessing the impact of environmental factors, natural disasters, or human interventions on heritage sites.

However, real-time integration presents several challenges, including data consistency, quality control, and computational efficiency. To address these, automated filtering techniques could be implemented to eliminate low-quality or irrelevant data, ensuring that only the most relevant images contribute to model updates [24, 44]. Additionally, AI-driven image selection could prioritize images with optimal viewpoints and lighting conditions, enhancing the accuracy of reconstructions.

Another crucial aspect is multi-temporal dataset fusion, as integrating data collected at different times can lead to geometric inconsistencies. Robust data fusion algorithms, such as deep learning-based feature matching and statistical normalization techniques, could minimize these distortions and improve the temporal accuracy of reconstructions [23, 26, 45].

Furthermore, cloud-based processing frameworks could significantly enhance computational efficiency, enabling scalable and near-real-time 3D reconstructions. By distributing the computational workload across cloud servers, large-scale cultural heritage sites could be reconstructed with minimal latency [46]. Future studies should focus on integrating these advanced methodologies to develop real-time, automated, and scalable 3D reconstruction systems for cultural heritage preservation.

Table 3. Statistics of the distribution of the M3C2 differences of the structures

Cultural Heritage	Reference Model	Compared Model	The Matched Point Numbers		The Percentages (%)			
			Incomparable	Compared	±1σ	±2σ	±3σ	≥±3σ
Holy Trinity Column	MP-1C	MP-1A	5,795	1,081,220	89.88	96.59	97.70	2.30
		MP-2A	7,174	1,079,841	91.92	96.21	97.23	2.77
		MP-2C	3,359	1,083,656	93.26	98.40	98.80	1.20
		MP-3A	14,132	1,072,883	93.17	96.86	97.78	2.22
		MP-3C	13,334	1,073,681	85.65	96.97	97.95	2.05
Roskilde Cathedral	MP-1C	MP-1A	53,315	2,270,134	89.41	98.46	98.95	1.05
		MP-2A	690,396	1,633,053	94.60	97.28	97.92	2.08
		MP-2C	122,141	2,201,308	91.35	96.27	98.16	1.84
		MP-3A	261,258	2,062,191	95.79	98.80	99.08	0.92
		MP-3C	58,879	2,264,570	86.08	94.93	97.32	2.68
Bode Museum	MP-1C	MP-1A	16,224	1,436,429	96.16	98.60	99.14	0.86
		MP-2A	16,067	1,436,586	95.70	98.47	99.10	0.90
		MP-2C	4,953	1,447,700	90.94	97.95	99.09	0.91
		MP-3A	29,234	1,423,419	93.34	98.14	99.09	0.91
		MP-3C	26,353	1,426,300	94.81	98.31	99.11	0.89
Petra	MP-1C	MP-1A	2,593	3,123,285	84.75	97.56	99.01	0.99
		MP-2A	1,861	3,124,017	96.30	98.94	99.45	0.55
		MP-2C	3,371	3,122,507	97.65	98.82	99.10	0.90
		MP-3A	9,287	3,116,591	96.41	98.18	98.78	1.22
		MP-3C	8,564	3,117,314	96.72	98.37	98.86	1.14

4. Conclusion

In today's digitalized information age, advances in science and technology contribute to the creation of highly accurate 3D inventories of cultural heritage. Cultural and natural heritage assets have significant value not only for the past but also for the transfer to future generations as entire tangible and intangible values, where the common history of the cohabiting communities and historical accumulations are revealed. In addition to the expected deterioration and destruction processes, unexpected and sudden occurrences such as war, terrorist attacks, and natural disasters may create circumstances that hinder the development of cultural heritage inventories. A multitude of projects to create cultural heritage inventories in areas that are under the threat of extinction and difficult to access due to the situations or even cultural heritages that no longer exist have been conducted with the crowdsourced data by collaboration with various non-governmental organizations and institutions. Based on our results, we recommend that future research focuses on refining the integrated methodology, standardizing data acquisition and processing protocols, and exploring innovative applications to enhance digital documentation and heritage preservation. These steps will support virtual museum initiatives and promote sustainable cultural heritage management.

Although publicly available social media images provide valuable resources for large-scale 3D reconstruction, their use introduces potential challenges related to privacy, data representation, and model accuracy. Firstly, privacy concerns arise when utilizing user-generated content without explicit consent, even when images are publicly shared. While this study strictly adheres to publicly available data, future research should integrate established ethical frameworks and legal guidelines to ensure responsible data usage and mitigate potential ethical issues. Secondly, the spatial and temporal distribution of social media images is inherently unbalanced, leading to biases in the reconstructed models. Popular tourist destinations are likely to have an abundance of images, whereas lesser-known sites may lack sufficient data for

reconstruction. This uneven data distribution impacts the completeness and accuracy of 3D models. Addressing these challenges requires further research into bias mitigation techniques and ethical data sourcing strategies. Lastly, several limitations should be acknowledged. Data acquisition constraints, including low image resolution, excessive filtering, lighting inconsistencies, seasonal variations, and inconsistent viewpoints, negatively affect reconstruction quality. Future studies could explore advanced filtering techniques and the integration of additional data sources to improve model completeness and accuracy. Additionally, this study does not incorporate deep learning-based super-resolution techniques, which could significantly enhance 3D reconstructions by refining details and improving feature extraction. Future research should consider integrating such methods to further improve the accuracy, visual quality, and reliability of reconstructed models.

Acknowledgement

This work has been supported by Yildiz Technical University Scientific Research Projects Coordination Unit under project number FBA-2023-5042. Duygu Arican is a Ph.D. scholarship holder from the Council of Higher Education (YÖK) in the field of "GIS and Informatic Applications", which is one of the 100 national priority areas determined by YÖK within the scope of the YÖK 100/2000 Doctorate Program.

Author contributions

Nursu Tunalioglu: Supervision, Conceptualization, Methodology, Writing-Reviewing and Editing., **Bahattin Erdogan and Taylan Ocalan:** Conceptualization, Validation of results, Writing-Original draft preparation., **Duygu Arican, Cemali Altuntas, Tumay Arda, Ali Hasan Dogan and Elif Zeynep Arikan:** Literature review, Data generation, Data interpretation, Visualization, Writing-Reviewing and Editing.

Conflicts of interest

The authors declare no conflicts of interest.

References

1. Halaç, H. H., & Bademci, F. (2021). Kültürel miras: Sistematik literatür incelemesi. *Safran Kültür ve Turizm Araştırmaları Dergisi*, *4*(2), 172-190.
2. Koller, D., Frischer, B., & Humphreys, G. (2010). Research challenges for digital archives of 3D cultural heritage models. *Journal on Computing and Cultural Heritage (JOCCH)*, *2*(3), 1-17.
3. Alyilmaz, C., Yakar, M., & Yilmaz, H. M. (2010). Drawing of petroglyphs in Mongolia by close range photogrammetry. Scientific Research and Essays, 5(11), 1216-1222.
4. Du, G., Zhou, M., Ren, P., Shui, W., Zhou, P., & Wu, Z. (2015, July). A 3D modeling and measurement system for cultural heritage preservation. In *International Conference on Optical and Photonic Engineering (icOPEN 2015)* (Vol. 9524, pp. 549-557). SPIE.
5. Gridan, M. R., Brebu, F. M., & Bala, A. C. (2014). Cultural heritage conserving using terrestrial laser scanning technology. In *14th International Multidisciplinary Scientific GeoConference SGEM 2014* (pp. 145-150).
6. Ulvi, A. (2020). Importance of unmanned aerial vehicles (UAVs) in the documentation of cultural heritage. *Turkish Journal of Engineering*, *4*(3), 104-112.
7. Kadobayashi, R., Kochi, N., Otani, H., & Furukawa, R. (2004). Comparison and evaluation of laser scanning and photogrammetry and their combined use for digital recording of cultural heritage. *International Archives of the Photogrammetry, Remote Sensing and Spatial Information Sciences*, *35*(5), 401-406.
8. Şasi, A., & Yakar, M. (2017). Photogrammetric modelling of sakahane masjid using an unmanned aerial vehicle. *Turkish Journal of Engineering*, *1*(2), 82-87.
9. Uslu, A., & Uysal, M. (2017). Arkeolojik eserlerin fotogrametri yöntemi ile 3 boyutlu modellenmesi: Demeter Heykeli örneği. *Geomatik*, *2*(2), 60-65.
10. Yakar, M., & Dogan, Y. (2018, November). 3D Reconstruction of residential areas with SfM photogrammetry. In *Conference of the Arabian Journal of Geosciences* (pp. 73-75). Cham: Springer International Publishing..
11. Varol, F. (2025). Creation of surface model using unmanned aerial vehicle (UAV) photogrammetry in cultural heritage areas: The example of Kilistra Ancient City. *International Journal of Engineering and Geosciences*, *10*(2), 137-150.
12. Yakar, İ., Çelik, M. Ö., Hamal, S. N. G., & Bilgi, S. (2021). Kültürel mirasın dokümantasyonu çalışmalarında farklı yazılımların karşılaştırılması: Dikilitaş (Theodosius Obeliski) Örneği. *Geomatik*, *6*(3), 217-226.
13. Inzerillo, L., & Santagati, C. (2016, October). Crowdsourcing cultural heritage: from 3D modeling to the engagement of young generations. In *Euro-Mediterranean Conference* (pp. 869-879). Cham: Springer International Publishing.
14. Mildenhall, B., Srinivasan, P. P., Tancik, M., Barron, J. T., Ramamoorthi, R., & Ng, R. (2021). Nerf: Representing scenes as neural radiance fields for view synthesis. *Communications of the ACM*, *65*(1), 99-106.
15. Dong, C., Loy, C. C., He, K., & Tang, X. (2015). Image super-resolution using deep convolutional networks. *IEEE transactions on pattern analysis and machine intelligence*, *38*(2), 295-307.
16. Snavely, N., Seitz, S. M., & Szeliski, R. (2006). Photo tourism: exploring photo collections in 3D. In *ACM siggraph 2006 papers* (pp. 835-846).

17. Agarwal, S., Snavely, N., Simon, I., & Seitz, S. M. (2009, September). andR. Szeliski. Building rome in a day. In *ICCV* (Vol. 1, No. 2, p. 7).
18. Herman, G. V., Caciora, T., Ilies, D. C., Ilies, A., Deac, A., Sturza, A., ... & Nistor, S. (2020). 3D Modeling of the Cultural Heritage: Between Opportunity and Necessity. *Journal of Applied Engineering Sciences*, *10*(1).
19. Deliry, S. I., & Avdan, U. (2024). Accuracy assessment of UAS photogrammetry and structure from motion in surveying and mapping. *International Journal of Engineering and Geosciences*, *9*(2), 165-190.
20. Bakirman, T., & Gumusay, M. U. (2020). Integration of custom street view and low-cost motion sensors. *International Journal of Engineering and Geosciences*, *5*(2), 66-72.
21. Grün, A., Remondino, F., & Zhang, L. (2004). Photogrammetric reconstruction of the great Buddha of Bamiyan, Afghanistan. *The Photogrammetric Record*, *19*(107), 177-199.
22. Grussenmeyer, P., & Al Khalil, O. (2017). From metric image archives to point cloud reconstruction: Case study of the Great Mosque of Aleppo in Syria. *The International Archives of the Photogrammetry, Remote Sensing and Spatial Information Sciences*, *42*, 295-301.
23. Alsadik, B. (2016). Crowdsource and web-published videos for 3D documentation of cultural heritage objects. *Journal of Cultural Heritage*, *21*, 899-903.
24. Somogyi, A., Barsi, A., Molnar, B., & Lovas, T. (2016). Crowdsourcing based 3D modeling. *The International Archives of the Photogrammetry, Remote Sensing and Spatial Information Sciences*, *41*, 587-590.
25. Alsadik, B. (2022). Crowdsource drone imagery–a powerful source for the 3D documentation of cultural heritage at risk. *International Journal of Architectural Heritage*, *16*(7), 977-987.
26. Stathopoulou, E. K., Georgopoulos, A., Panagiotopoulos, G., & Kaliampakos, D. (2015). Crowdsourcing lost cultural heritage. *ISPRS annals of the photogrammetry, remote sensing and spatial information sciences*, *2*, 295-300.
27. Griffiths, S., Edwards, B., Wilson, A., Labrosse, F., Miles, H., Roberts, J., & Tiddeman, B. (2015). Crowd-sourcing archaeological research: HeritageTogether digital public archaeology in practice. Internet Archaeology, 40. Retrieved October 12, 2023, from http://www.rekrei.org
28. Uslu, A., & Uysal, M. (2021). Kitle kaynaklı fotoğraflar kullanılarak kültürel mirasın üç boyutlu modellenmesi ve web tabanlı görselleştirilmesi: Afrodisias-Tetrapylon örneği. *Afyon Kocatepe Üniversitesi Fen Ve Mühendislik Bilimleri Dergisi*, *21*(3), 632-639.
29. Uslu, A., & Uysal, M. (2022). Kitle kaynaklı insansız hava aracı verileri kullanılarak ahşap eserlerin 3B modellenmesi: Truva Atı örneği. *Mobilya ve Ahşap Malzeme Araştırmaları Dergisi*, *5*(2), 155-166.
30. Kirillov, A., Mintun, E., Ravi, N., Mao, H., Rolland, C., Gustafson, L., ... & Girshick, R. (2023). Segment anything. In *Proceedings of the IEEE/CVF international conference on computer vision* (pp. 4015-4026).
31. Westoby, M. J., Brasington, J., Glasser, N. F., Hambrey, M. J., & Reynolds, J. M. (2012). 'Structure-from-Motion'photogrammetry: A low-cost, effective tool for geoscience applications. *Geomorphology*, *179*, 300-314.
32. Iglhaut, J., Cabo, C., Puliti, S., Piermattei, L., O'Connor, J., & Rosette, J. (2019). Structure from motion photogrammetry in forestry: A review. *Current Forestry Reports*, *5*(3), 155-168.
33. Yang, M. D., Chao, C. F., Huang, K. S., Lu, L. Y., & Chen, Y. P. (2013). Image-based 3D scene reconstruction and exploration in augmented reality. *Automation in Construction*, *33*, 48-60.
34. Favalli, M., Fornaciai, A., Isola, I., Tarquini, S., & Nannipieri, L. (2012). Multiview 3D reconstruction in geosciences. *Computers & Geosciences*, *44*, 168-176.
35. Carrivick, J. L., Smith, M. W., & Quincey, D. J. (2016). *Structure from Motion in the Geosciences*. John Wiley & Sons.
36. Snavely, N., Seitz, S. M., & Szeliski, R. (2008). Modeling the world from internet photo collections. *International journal of computer vision*, *80*(2), 189-210.
37. Lague, D., Brodu, N., & Leroux, J. (2013). Accurate 3D comparison of complex topography with terrestrial laser scanner: Application to the Rangitikei canyon (NZ). *ISPRS journal of photogrammetry and remote sensing*, *82*, 10-26.
38. DiFrancesco, P. M., Bonneau, D., & Hutchinson, D. J. (2020). The implications of M3C2 projection diameter on 3D semi-automated rockfall extraction from sequential terrestrial laser scanning point clouds. *Remote Sensing*, *12*(11), 1885.
39. Haugen, B. D. (2016). *Qualitative and quantitative comparative analyses of 3D lidar landslide displacement field measurements*. Colorado School of Mines.
40. Esposito, G., Mastrorocco, G., Salvini, R., Oliveti, M., & Starita, P. (2017). Application of UAV photogrammetry for the multi-temporal estimation of surface extent and volumetric excavation in the Sa Pigada Bianca open-pit mine, Sardinia, Italy. *Environmental Earth Sciences*, *76*(3), 103.
41. UNESCO. (1972). Convention Concerning the Protection of The World Cultural and Natural Heritage, adopted by the General Conference at its seventeenth session, Paris, 16 November 1972.
42. Gautier, Q. K., Garrison, T. G., Rushton, F., Bouck, N., Lo, E., Tueller, P., ... & Kastner, R. (2020). Low-cost 3D scanning systems for cultural heritage documentation. *Journal of Cultural Heritage Management and Sustainable Development*, *10*(4), 437-455.

43. Doulamis, A., Voulodimos, A., Protopapadakis, E., Doulamis, N., & Makantasis, K. (2020). Automatic 3d modeling and reconstruction of cultural heritage sites from twitter images. *Sustainability*, *12*(10), 4223.
44. Llull, C., Baloian, N., Bustos, B., Kupczik, K., Sipiran, I., & Baloian, A. (2023). Evaluation of 3d reconstruction for cultural heritage applications. In *Proceedings of the IEEE/CVF international conference on computer vision* (pp. 1642-1651).
45. Jaramillo, P., & Sipiran, I. (2024, September). Cultural heritage 3d reconstruction with diffusion networks. In *European Conference on Computer Vision* (pp. 104-117). Cham: Springer Nature Switzerland.
46. Hadjiprocopis, A., Wenzel, K., Rothermel, M., Ioannides, M., Fritsch, D., Klein, M., ... & Santos, P. (2014). Cloud-based 3D Reconstruction of Cultural Heritage Monuments using Open Access Image Repositories. In *GCH (Short and Project Papers)*.